GLOBAL VARIABILITY & CHANGES IN OCEAN TOTAL ALKALINITY FROM AQUARIUS SATELLITE

Rana A. Fine, Debra A. Willey and Frank J. Millero

Rosenstiel School, University of Miami

4600 Rickenbacker Cswy, Miami, FL 33149 USA

UNIVERSITY OF MIAMI
ROSENSTIEL
SCHOOL of MARINE &
ATMOSPHERIC SCIENCE

AQUARIUS/SAC-D

Introduction

The unprecedented salinity coverage from the Aquarius satellite provides the opportunity to calculate surface alkalinity globally. In the ocean, total alkalinity (TA) is a gauge of the ability of seawater to neutralize acids. TA can be measured on seawater samples, and is defined as

$$TA = [HCO_3^-] + 2[CO_3^{2-}] + [B(OH)_4^-] + \text{other minor bases}$$

There is a strong correlation between surface ocean TA and salinity (Broecker and Peng, 1982; Millero et al., 1998 a, b; Lee et al., 2006) (Figs. 1a and b). Processes affecting TA include addition of freshwater by precipitation and sea ice melting, mixing, and removal during evaporation and sea ice formation. Non-conservative behavior has been shown to affect TA, specifically production of $CaCO_3$ that reduces TA and dissolution of $CaCO_3$ that increases TA (Bates et al., 1996; Winn et al., 1998).

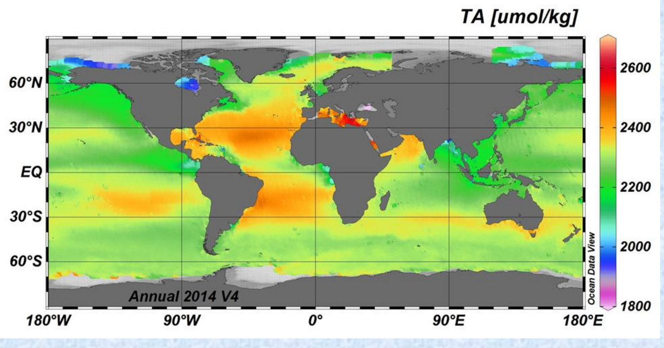

Figure 1a. TA (μmol/kg) annual averaged 2014 using Aquarius SSS and Reynolds SST.

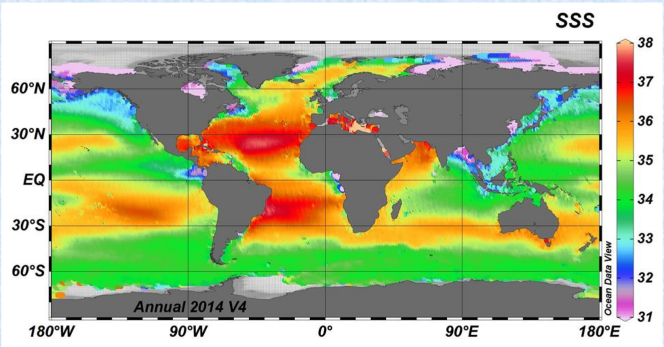

Figure 1b. SSS annual averaged 2014 from Aquarius SSS.

In the subtropics, the salinity maximum zones correspond to regions of maximum TA. Toward the equator and higher latitudes, TA generally decreases with decreasing salinity. TA shows a positive correlation with SSS over the ocean except perhaps for the Arctic low salinity waters and Southern Ocean where there is upwelling of TA enriched waters (Key et al., 2004).

Empirical relationship between TA, SSS and SST

In earlier work (Lee et al., 2006), the ocean was divided into five regions where an empirical relationship was used to represent surface TA as a function of SST and SSS.

$$TA = a + b\,(SSS - 35) + c\,(SSS - 35)^2 + d\,(SST - 20) + e\,(SST - 20)^2,$$

where the coefficients a-e are defined for five ocean regions: the subtropics (30°N-30°S), Pacific equatorial upwelling, North Atlantic (30°-80°N), North Pacific (≥30°N, and including a term for longitude), and Southern Ocean (30°-70°S). Note that in the subtropics, where we focus later on longer term trends, only 2.4% of grid pints fall out of range of Lee et al. empirical relationship.

Ground Truthing Satellite TA data

Satellite derived TA and salinity are compared to recent ocean observations at BATS and HOTS (Figs. 2a and b) (Bates et al., 1996; Winn et al., 1998). Differences are well within the errors of the satellite TA of ± 17 μmol/kg, except for late winter 2012 at HOTS. Differences are related to salinity differences, which may be due to distances between *insitu* stations and satellite points.

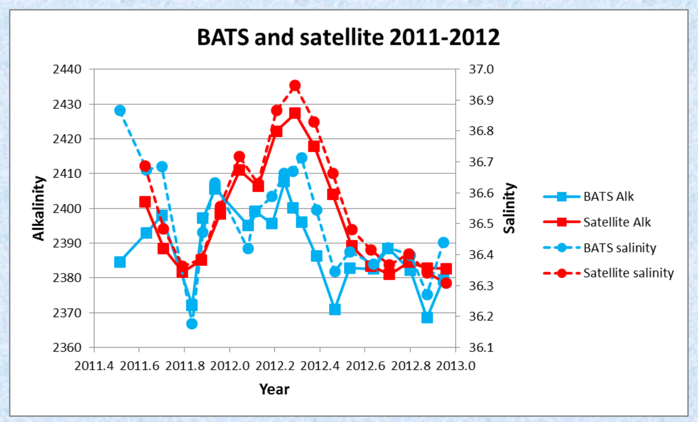

Figure 2a. TA and salinity for BATS station (32.0°N, 64.0°W) and satellite (Aquarius location 31.5°N, 64.5°W). Analytical error in measurement of TA (± 1.2 μmol/kg).

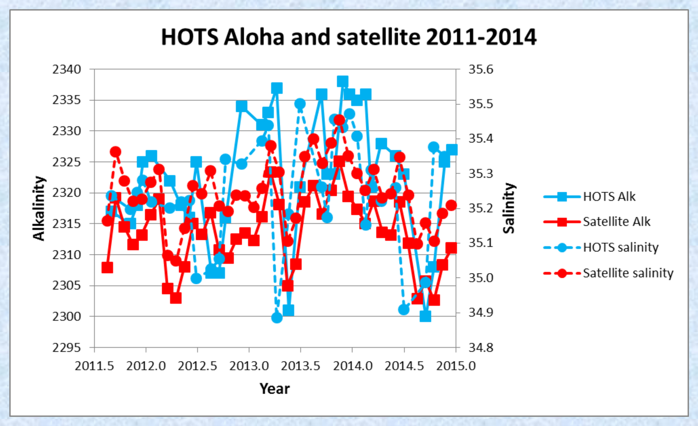

Figure 2b. TA and salinity for HOTS station (22.75°N, 158.0°W) and satellite (Aquarius location 22.5°N, 158.5°W).

Satellite Data and Errors

A motivation for using satellite data is that there are special challenges for understanding the carbon system in high latitudes. One such challenge is scarcity of carbon data. From August 2011 to June 2015, Aquarius continuously collected and distributed SSS data. We are using Aquarius Version 4.0, (Lagerloef et al., 2015), L3 mapped product, with a spatial resolution of 1°, smoothed monthly. For SST, we are using NOAA OI.v2 SST monthly fields 1x1° grid (Reynolds, et al., 2002). These data are providing, for the first time, an opportunity to document spatial and temporal variability in surface TA. The following errors are contributing to satellite TA: satellite SSS bias ±11 μmol/kg, Lee et al. (2006) empirical relationship ± 8.1 μmol/kg, and averaging errors due to eddies ~±10 μmol/kg. Taking the square root of the sum of the squares of these errors gives ~±17 μmol/kg error in satellite derived TA. This greatly exceeds the uncertainty of analytical measurements of ± 1.2 μmol/kg.

Spatial variability

Maps that show the difference between the 2014 annual average TA and SSS at each grid point minus the global annual average, respectively, of TA = 2299 and SSS = 34.646, are shown in Figs. 3a, and b. Differences can exceed ±200 μmol/kg for TA, or about ±9%, and ±5 for SSS, or about ±14%. With over 33,000 ocean grid points, < 2% fall outside the range for TA ±200 μmol/kg, and < 2% fall outside the range for SSS ±5. It is clear from these maps that spatial variations in TA are highly correlated with spatial variations in SSS. The TA and SSS differences from a global annual average are considerably larger in the high latitude northern than southern hemisphere. In addition, these spatial variations greatly exceed seasonal temporal variations.

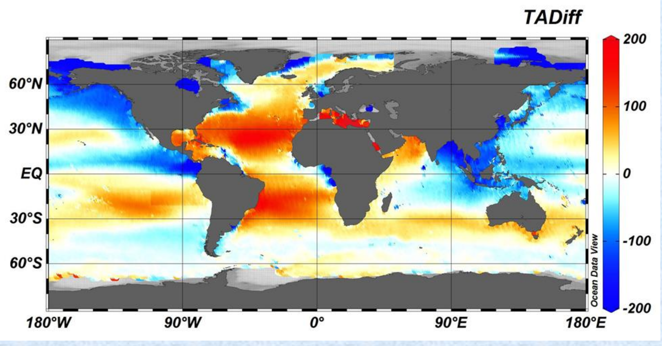

Figure 3a. Map of 2014 annual average at each grid point minus global 2014 annual average TA of 2299 μmol/kg using satellite SSS and SST.

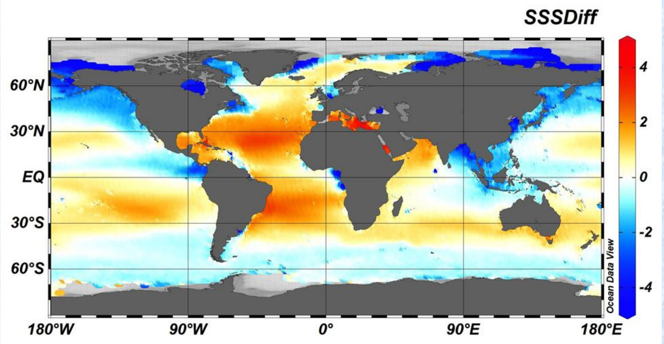

Figure 3b. Map of 2014 annual average at each grid point minus global 2014 annual average SSS of 34.646 using Aquarius SSS.

Temporal Variability

The magnitude of temporal variability in TA is documented for time scales of seasons to years. The seasonal amplitude for 2014 from satellite data is calculated by differencing at each grid point monthly mean TA (Fig. 4a) and SSS (Fig. 4b) maximum minus minimum. The seasonal amplitude in TA for 2014 is as large as 100 μmol/kg or less than 5% of the mean, and in SSS it is 4. The percentage exceeding 100 μmol/kg for TA is <5%, and exceeding 4 for SSS is <1%. Largest seasonal amplitudes in TA are observed in the high latitudes, tropical Pacific and Atlantic and coastal regions. In these regions there are the largest seasonal amplitudes in SSS due to seasonal changes in precipitation, evaporation, run off, and melting and freezing of ice.

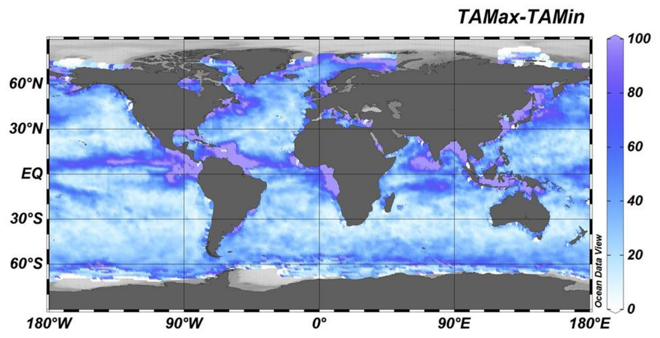

Figure 4a. Seasonal amplitude of TA(μmol/kg) from 2014 satellite data, difference between the maximum and minimum applied to monthly mean TA at each grid point.

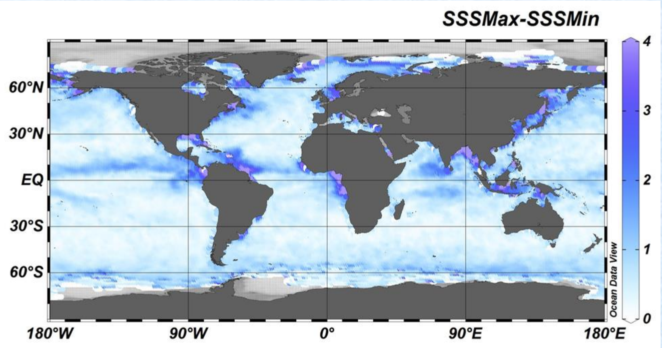

Figure 4b. Seasonal amplitude of SSS from 2014 satellite data, difference between the maximum and minimum applied to monthly mean SSS at each grid point.

In an earlier study, Aquarius SSS and World Ocean Data [Conkwright et al., 2002] (WOD) for 2011-2013 compare well [Reagan et al., 2014]. Negative biases for Aquarius observed from 25°S to 25°N change to positive biases in higher latitudes. Other reported biases for the version 4.0 Aquarius SSS are mostly in the northern and southern high latitudes, and close to the coast on eastern and western sides of continents [Lagerloef and Kao, 2015]. Here satellite derived 2014 TA are compared to WOD 2014 to test the accuracy of the satellite data for the purpose of inferring longer time trends (Fig. 5a shows TA, WOD includes only data from 2014). For example, largest differences exceeding ±20 μmol/kg are observed in mid-latitude coastal regions around North America and show relatively high TA (and salinity, not shown) in 2014 satellite data, while around Asia TA (and salinity) in 2014 are low. These areas with large differences between 2014 satellite and in situ data will not be considered when analyzing at longer term trends.

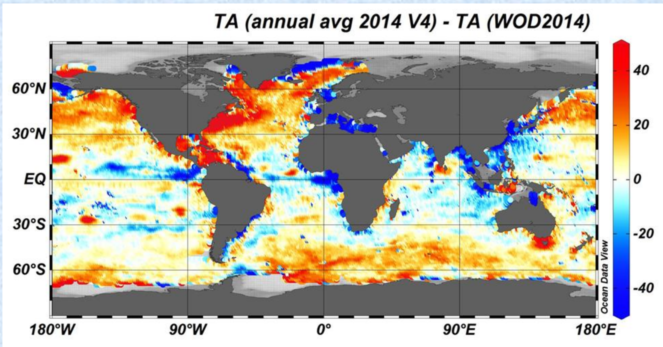

Figure 5a. Difference between annual averaged satellite derived TA (μmol/kg) in 2014 and WOD 2014 (2014 data).

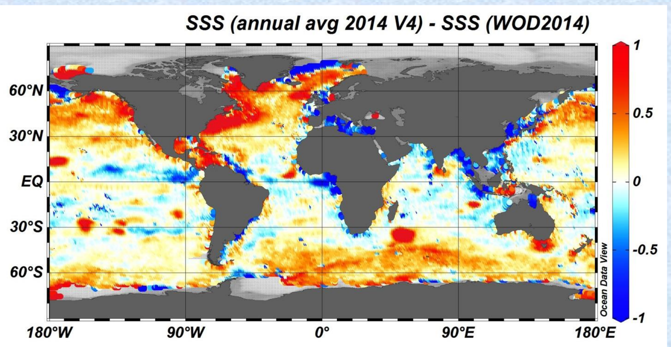

Figure 5b. Difference between annual averaged satellite derived SSS in 2014 and WOD 2014 (2014 data).

Longer Term Trends

To infer longer term trends, annual averaged differences in TA between 2014 satellite and WOD 1975-84 [Conkwright et al., 2002] are compared at each grid point (Fig. 6). WOD7584 is the World Ocean Data including data from 1975 through 1984. Maximum difference in TA is ~±50 μmol/kg, which is about three times the global RMS for the version 4.0 Aquarius derived TA data. With over 33,000 ocean grid points, <6% of grid points fall outside of this range. Patterns are highly correlated with SSS differences. There are similarities in patterns of the differences between satellite TA 2014 and both WOD 2014 and WOD7584, again related to biases in version 4.0 Aquarius data. For this reason in the comparison with climatology, we concentrate on regions where biases in Aquarius are less than ±20 μmol/kg.

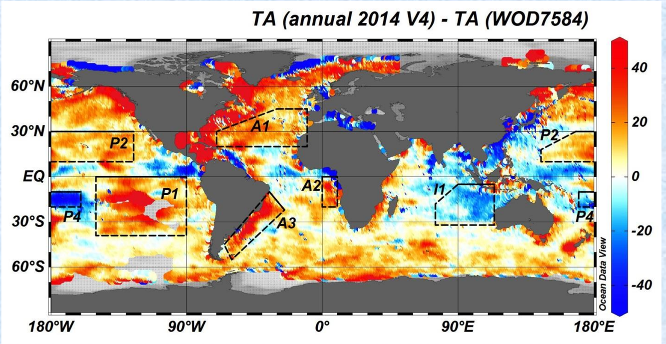

Figure 6a. Difference between annual averaged satellite derived TA (μmol/kg) in 2014 and WOD 1975-84. Boxes are regions where there are significant changes in TA over the several decades. Note there is no box P3.

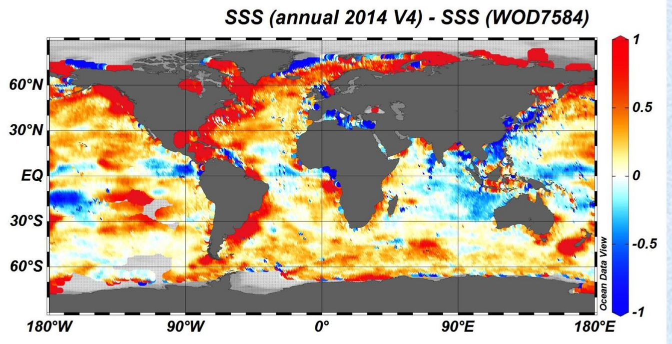

Figure 6b. Difference between annual averaged satellite derived SSS in 2014 and WOD 1975-84.

It is important to note that large scale differences between satellite 2014 TA and WOD7584 appear consistent with climate related changes in ocean SSS. Over the past fifty years as the ocean has warmed, there has been an amplification of inter-basin surface salinity differences, e.g., subtropical cells getting saltier and high latitudes getting fresher due to increased sea ice melt and increased precipitation [Curry et al., 2003; Schmidt, 2008; Durack and Wijffels, 2010]. Melzer and Subrahmanyam [2015] find an average increase in salinities of subtropical gyres of 0.12 over 61 years to 2010. When comparing 2014 satellite salinity and WOD7584 salinity has increased by more than 1 at grid points in the subtropical gyres (not shown). The increases in TA in subtropical gyres are consistent with increased salinity. At temperatures and salinities of subtropical surface waters, a change of 1 in salinity (keeping temperature constant) is about a 50 μmol/kg change in TA. Looking in 1°x1° squares between 1975-84 and 2014 TA increases exceed the satellite error of ±20 μmol/kg in most tropical and subtropical regions (Fig. 6): North Atlantic (A1), eastern (A2) and western South Atlantic (A3), and eastern South Pacific (P1). In these four subtropical regions (A1-3 and P1, Fig. 6), between 25 and 40% of TA have increased by 20-50 μmol/kg, and in A3 13-14% of TA have increased by at least 50 μmol/kg. In the North Pacific (P2), 15 % of TA has increased by 20-50 μmol/kg. In addition, the western subtropical South Atlantic coincident with the warm and salty poleward flowing Brazil Current is higher in TA.

In the opposite vein, in the southeast Indian (I1) and tropical southwest Pacific (P4), 17 and 57%, respectively, of TA have decreased between 1975-84 and 2014 by 20-50 μmol/kg. In 2014, waters fresher and lower in TA in the southeastern Indian subtropics (I1) could be due to increased Pacific to Indian throughflow. During El Nino there is weaker throughflow of fresher Pacific waters [Gordon and Fine, 1996]. The year 2014 was a neutral to mild La Nina year, which implies stronger throughflow of fresher Pacific waters into the South Indian, while the decade 1975-84 contained three El Nino's and the 1982-83 one was strong suggesting weaker throughflow during the decade.

The uptake by the ocean of CO_2 does not change the TA of seawater, but it does increase the absolute salinity of seawater [Woosley et al., 2014]. Changes in boundaries between ocean regions, for example between polar and subtropical regions, and changes in mixing due to changes in stratification and changing currents are also likely to affect the carbon system. Increasing surface TA in subtropical regions from increasing salinity and temperature related to climate change causes the saturation states of calcite and aragonite to decrease, i.e., these minerals are more soluble [e.g., Feely et al., 2012]. The increase in temperature and salinity of seawater can change the carbon dioxide system of average surface waters (S=35, pH=8.1, TA = 2300 μmol/kg, TCO_2=1961 μmol/kg). For example (Lewis and Wallace, 1998), the combined changes in temperature from 25 to 27°C and salinity from 35 to 37 cause the pH to decrease by -0.055; the pCO_2 to increase by 47 μatm, and the saturation state of calcite (Ω) and aragonite to decrease, respectively by -0.13 and -0.05. Thus, ocean acidification is increasing from anthropogenic CO_2 dissolving in ocean, and in the subtropics from temperature and salinity increasing. Based on increasing TA in the subtropical regions over the past few decades, it is expected that it is becoming more difficult for calcifying organisms to make their shells.

Conclusions

The SSS satellite coverage by Aquarius has provided an unprecedented opportunity to assess variability in surface TA over the global ocean. Spatial and temporal variability in TA are mostly due to variability in salinity. Spatial variability in TA and salinity exceed, by an order of magnitude, temporal variability – including seasonal and comparison with climatological data. The northern hemisphere has the most spatial variability in TA and salinity, while reduced variability in Southern Ocean TA is due to less salinity variability and upwelling of waters enriched in TA. For the first time, comparison of recent satellite derived TA with that from climatological data shows that TA has been increasing in high evaporative subtropical regions, which is consistent with what is known about changes in the global water cycle. Anthropogenic CO_2 dissolving in the ocean is increasing ocean acidification, and here we show in the subtropics it is increasing from increasing temperature and salinity. Based on increasing TA in the subtropical regions over the past few decades, it is expected that it is becoming more difficult for calcifying organisms there to make their shells. This work is a step toward providing a global baseline for TA that can be used to compare future data, and for evaluating spatial and temporal variability and past trends. Due to the large spatial variability, to evaluate changes in TA due to, for example changes in the global water cycle, it will be important to have high resolution spatial coverage as can be achieved from satellite..

References

Bates, N.R., A.F. Michaels, and A.H. Knap, 1996. Alkalinity changes in the Sargasso Sea: geochemical evidence of calcification? *Mar. Chem.*, 51, 347-358.

Broecker, W.S., and T.H. Peng, 1982. *Tracers in the Sea*, Published by Lamont-Doherty Geological Observatory, Columbia University.

Conkwright, M. E., J. I. Antonov, O. Baranova, T. P. Boyer, H. E. Garcia, R. Gelfeld, D. Johnson, R. A. Locarnini, P. P. Murphy, T. D. O'Brien, I. Smolyar, and C. Stephens (2002), *World Ocean Data Base 2001, vol. 1: Introduction*, S. Levitus, Ed., *NOAA Atlas NESDIS 42*, 167 pp. (National Oceanic and Atmospheric Administration, Silver Spring, MD) .

Curry, R., B. Dickson, and I. Yashayaev (2003), A change in the freshwater balance of the Atlantic Ocean over the past four decades, *Nature* **426**, 826-829.

Durack, P. J., and S. E. Wijffels (2010), Fifty-year trends in global ocean salinities and their relationship to broad scale warming. *J. Clim*. **23**, 4342-4362.

Feely, R. A., C. L. Sabine, R. H. Byrne, F. J. Millero, A. G. Dickson, R. Wanninkhof, A. Murata, L. A. Miller, and D. Greeley (2012), Decadal changes in the aragonite and calcite saturation state of the Pacific Ocean. *Gl. Biogeochem. Cycles* **26**, GB3001, doi:10.1029/2011GB004157.

Gordon, A. L., and R. A. Fine (1996), Pathways of water between the Pacific and Indian oceans in the Indonesian Seas, *Nature* **379**, 146-149.

Key, R.M., A. Kozyr, C.L. Sabine, K. Lee, R. Wanninkhof, J.L. Bullister, R.A. Feely, F.J. Millero, C. Mordy and T.-H. Peng. 2004. A global ocean carbon climatology: Results from Global Data Analysis Project (GLODAP). *Gl. Biogeochem. Cycles* 18, GB4031, doi:10.1029/2004GB002247.

Lagerloef, G., and H.- Y. Kao (2015), Aquarius salinity validation analysis version 4.0,podaac.jpl.nasa.gov/SalinityDensity/aquarius/docs/v4/AQ-014-PS-0016_AquariusSalinityDataValidationAnalysis_DatasetVersion4.0and3.0.pdf.

Lagerloef et al. 2014. Aquarius salinity validation analysis version 3.0, AQ-014-PS-0016.

Lee, K., L.T. Tong, F.J. Millero, C.L. Sabine, A.G. Dickson, C. Goyet, G.-H. Park, R. Wanninkhof, R.A. Feely, and R.M. Key. 2006. Global relationships of total alkalinity with salinity and temperature in surface waters of the world's ocean. *Geophys. Res. Lett.* 33, L19605, doi:10.1029/2006GL027207.

Lewis, E., and D. W. R. Wallace (1998), Program developed for CO2 system calculations, Rep. 105, 33 pp., Oak Ridge Natl. Lab., Oak Ridge, Tenn. [Available at http://cdiac.esd.ornl.gov/oceans/co2rprt.html]

Melzer, B. A., and B. Subrahmanyam(2015), Investigating decadal changes in sea surface salinity in oceanic subtropical gyres. *Geophys. Res. Lett*. **42**, doi:10.1002/2015GL065636.

Millero, F.J, Lee, K. and Roche, M.P., 1998a. Distribution of alkalinity in the surface waters of the major oceans, *Mar. Chem*., 60, 111-130.

Millero, F.J, et al. 1998b. Assessment of the quality of the shipboard measurements of total alkalinity on the WOCE hydrographic program Indian Ocean CO_2 survey cruises 1994-1996, *Mar. Chem*., 63, 9-20.

Reagan, J., T. Boyer, J. Antonov, and M. Zweng (2014), Comparison analysis between Aquarius sea surface salinity and World Ocean Database in situ analyzed sea surface salinity, *J. Geophys. Res. Oceans* **119**, 8122-8140, doi:10.1002/2014JC009961 (2014).

Reynolds, R.W., N.A. Rayner, T.M. Smith, D.C. Stokes, and W. Wang, 2002: An Improved In Situ and Satellite SST Analysis for Climate, J. Climate, Vol 15. The paper is available in Adobe Acrobat in the directory: ftp://ftp.emc.ncep.noaa.gov/cmb/sst/papers/oiv2pap/).

Schmidt, R. W. (2008), Salinity and the global water cycle, *Oceanogr*, 21, 12-19.

Winn, C.D., Y.-H. Li, F.T. Mackenzie, D.M. Karl, 1998. Rising surface ocean dissolved inorganic carbon at the Hawaii Ocean Time-series site, *Mar. Chem*., 60, 33-47.

Woosley, R. J., F. Huang, and F. J. Millero (2014), Estimating absolute salinity (S_A) in the world's oceans using density and composition, *Deep-Sea Res. I* 93, 14-20.

Acknowledgement This project is funded by NASA grant NNX13AE11G.